J. Cent. South Univ. (2018) 25: 2688−2700
DOI: https://doi.org/10.1007/s11771-018-3946-x

Springer

Dynamic probabilistic design technique for multi-component system with multi-failure modes

ZHANG Chun-yi(张春宜)[1], LU Cheng(路成)[1, 2], FEI Cheng-wei(费成巍)[3],
JING Hui-zhe(井慧哲)[1], LI Cheng-wei(李成伟)[1]

1. School of Mechanical and Power Engineering, Harbin University of Science and Technology, Harbin 150080, China;
2. School of Aeronautics, Northwestern Polytechnical University, Xi'an 710072, China;
3. Department of Aeronautics and Astronautics, Fudan University, Shanghai 200433, China

Abstract: For unacceptable computational efficiency and accuracy on the probabilistic analysis of multi-component system with multi-failure modes, this paper proposed multi-extremum response surface method (MERSM). MERSM model was established based on quadratic polynomial function by taking extremum response surface model as the sub-model of multi-response surface method. The dynamic probabilistic analysis of an aeroengine turbine blisk with two components, and their reliability of deformation and stress failures was obtained, based on thermal-structural coupling technique, by considering the nonlinearity of material parameters and the transients of gas flow, gas temperature and rotational speed. The results show that the comprehensive reliability of structure is 0.9904 when the allowable deformations and stresses of blade and disk are 4.78×10^{-3} m and 1.41×10^{9} Pa, and 1.64×10^{-3} m and 1.04×10^{9} Pa, respectively. Besides, gas temperature and rotating speed severely influence the comprehensive reliability of system. Through the comparison of methods, it is shown that the MERSM holds higher computational precision and speed in the probabilistic analysis of turbine blisk, and MERSM computational precision satisfies the requirement of engineering design. The efforts of this study address the difficulties on transients and multiple models coupling for the dynamic probabilistic analysis of multi-component system with multi-failure modes.

Key words: probabilistic analysis; multi-extremum response surface method; multi-component; multi-failure modes

Cite this article as: ZHANG Chun-yi, LU Cheng, FEI Cheng-wei, JING Hui-zhe, LI Cheng-wei. Dynamic probabilistic design technique for multi-component system with multi-failure modes [J]. Journal of Central South University, 2018, 25(11): 2688–2700. DOI: https://doi.org/10.1007/s11771-018-3946-x.

1 Introduction

Complex structure always comprises multiple components (or sub-components) [1]. The structure is commonly regarded as an assemblage in mechanical system, which directly determines the working performance and safety of whole system [2]. Under the effect of complex loads, multiple failure modes potentially occur for many components during the operation of mechanical system. Therefore, the design and analysis of complex structure involves multiple components and multi-failure modes. Effective design and

Foundation item: Projects(51275138, 51605016) supported by the National Natural Science Foundation of China; Project(12531109) supported by the Science Foundation of Heilongjiang Provincial Department of Education, China; Project supported by Research Start-up Funding of Fudan University, China
Received date: 2017-09-14; **Accepted date:** 2018-04-19
Corresponding author: FEI Cheng-wei, PhD; E-mail: cwfei@fudan.edu.cn; ORCID: 0000-0001-5333-1055

analysis of multi-component system with multi-failure modes hold a great signification for the development of mechanical system [3]. Despite of a large number of studies on the analysis of the system from a deterministic perspective at present [4–6], the design accuracy is unacceptable because of neglecting the randomness of design variables. To accurately design multi-component system with multi-failure modes, it is urgent to perform dynamic reliability analysis of this system from a probabilistic perspective considering multi-failure modes of sub-component, the randomness of design variables and the transient of mechanical loads [3].

The reliability analysis of single structure or single mode is the basis of probabilistic analysis of multi-component system. Monte Carlo (MC) method [2, 7–9] and traditional response surface methods (RSMs) [10–12] are two main approaches for structural reliability analysis. Nevertheless, it is difficult for the two techniques to cater for the analysis and computation problem of large-scale system with multiple components, especially for reliability analysis problem. Recently, a large number of advanced RSMs have emerged. ZHANG et al [13] proposed extremum RSM for two-link flexible robot manipulator; REN et al [14] discussed neural network RSM for structural reliability analysis; ZHAO et al [15] studied the Kriging model for structural reliability analysis; References [16–20] focused on support vector machine RSM for reliability analysis and the method was further applied to the probabilistic design and analysis of aeroengine typical components; BAI et al [21] also adopted probabilistic approaches to complete the dynamic probabilistic analysis of stress and deformation for aeroengine blisk assemblies.

Along with the rapid development of high performance and high reliability of complex machinery just like an aeroengine, however, the probabilistic analysis of multi-component system attracts the attention of many researchers so that new techniques and methods for probabilistic analysis have got a rapid development. FEI et al [3, 22] proposed distributed collaborative RSM and distributed collaborative extremum RSM for the dynamic assembly reliability analysis and design of turbine blade radial running clearance; ZHAI et al [23] also presented multi-response surface model (MRSM) for the reliability sensitivity analysis of turbine blade-tip clearance. Although these efforts studied the probabilistic analysis of multi-component system by different methods and the precision and efficiency of calculation get a large improvement, most of methods only finish the probabilistic analysis of single-component or single-failure mode. Although some models and methods are used to handle the probabilistic analysis of multi-component and multi-failure for complex structure, their computational efficiency and accuracy need to be improved because the transients of probabilistic analysis were not commendably handled. With respect to the above heuristic thought of ERSM [16–20] and MRSM [23], it is promising to deal with the problems of transients and many models in the probabilistic analysis of multi-component structure system with multi-failure mode.

The objective of this study attempts to develop multi-extremum response surface method (MERSM) by combining the thoughts of ERSM and MRSM to carry out the dynamic probabilistic analysis of multi-component system with multi-failure modes. Regarding the study case of the comprehensive reliability analysis of an aeroengine turbine blisk by considering the failure modes of deformations and stresses for turbine blade and turbine disk, nonlinear material property and time-varying loads, the validity and feasibility of MERSM are verified. Besides, the impact probabilities of input random variables on the reliability of blisk structure are achieved.

In what follows, in Section 2 MERSM is studied in detail including ERSM, MRSM and the mathematical model of MERSM, to resolve the transients and multiple models in the probabilistic analysis of multi-failure modes and multi-component system. Section 3 discusses the approaches of dynamic probabilistic analysis comprising computational methods of reliability and sensitivity by using MERSM. The dynamic probabilistic analysis of blisk, an assemblage, including two components (blade and disk) and two failure modes (deformation and stress) is accomplished to validate the proposed MERSM in Section 4. Section 5 gives the summarized

conclusions of this study.

2 Basic theory

This section introduces the basic principle and model of ERSM, and then expands it to MERSM for multi-component multi-failure modes probabilistic design.

2.1 Extremum response surface method, ERSM

2.1.1 ERSM principle

In dynamic probabilistic analysis, ERSM merely calculates a single extreme value of transient output responses rather than all values under different input vectors within a time domain [0, T], which is equivalent to transforming a stochastic process into a random variable for output response [3, 13, 17].

ERSM simplifies the time-varying (process) output response of the dynamic probabilistic analysis of single component (structure) or single failure mode into the extremum output response of dynamic analysis [13]. In other words, the extremum value of transient process of output response is selected as a new response of dynamic analysis to build response surface function (also called extremum response surface function) and execute the dynamic probabilistic analysis of structural response. Due to only considering the extremum value of output response, this method is efficient to reduce computational cost and improve computational precision on probabilistic analysis [18–20].

2.1.2 ERSM model

The basic principle of ERSM is shown in Figure 1. With the jth input vector variables $\boldsymbol{X}^{(j)}$, the extremum of output response $y^{(j)}(t, \boldsymbol{X}^{(j)})$ is $y_{\max}^{(j)}(\boldsymbol{X}^{(j)})$ in the time domain [0, T]. The data set $\{y_{\max}^{(j)}(\boldsymbol{X}^{(j)}): j=1, 2, \cdots, k\}$ consisting of the maximum output responses is used to fit the extremum response curve $y(\boldsymbol{X})$ [18, 20]:

$$y(\boldsymbol{X}) = f(\boldsymbol{X}) = \left\{ y_{\max}^{(j)}\left(\boldsymbol{X}^{(j)}\right): j=1, 2, \cdots, r \right\} \tag{1}$$

where $f(\boldsymbol{X})$ is an extremum response surface equation; r is the number of sample vectors.

The ERSM is used to fit an extremum response surface to a series of nonlinear dynamic analyses by simulating the real limit-state surface and the quadratic polynomial function [21, 22]. The

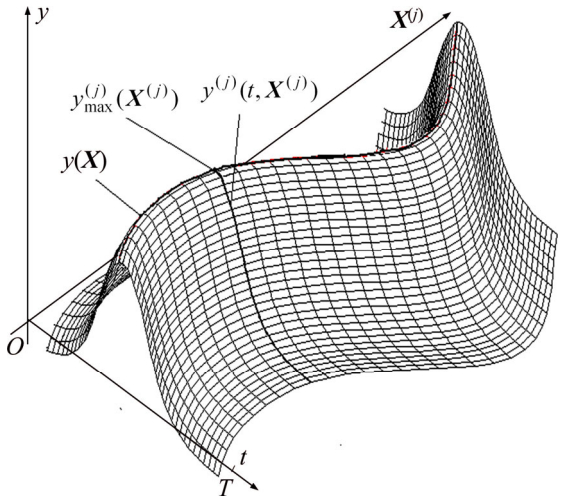

Figure 1 Basic principle of ERSM

response surface function is expressed by

$$y(\boldsymbol{X}) = A + \boldsymbol{B}\boldsymbol{X} + \boldsymbol{X}^{\mathrm{T}}\boldsymbol{C}\boldsymbol{X} \tag{2}$$

in which A, $\boldsymbol{B}$ and $\boldsymbol{C}$ are the constant coefficient, the vector of linear term coefficients and the matrix of quadratic term coefficients, respectively, and are expressed as

$$\boldsymbol{B} = \begin{bmatrix} b_1 & b_2 & \cdots & b_k \end{bmatrix} \tag{3}$$

$$\boldsymbol{C} = \begin{bmatrix} c_{11} & & & & \\ c_{21} & c_{22} & & & \\ c_{31} & c_{32} & c_{33} & & \\ \vdots & \vdots & \vdots & \ddots & \\ c_{k1} & c_{k2} & c_{k3} & \cdots & c_{kk} \end{bmatrix} \tag{4}$$

$$\boldsymbol{X} = \begin{bmatrix} X_1^{(j)} & X_2^{(j)} & \cdots & X_k^{(j)} \end{bmatrix}^{\mathrm{T}} \tag{5}$$

where k is the number of input random variables.

2.2 Multi-extremum response surface method, MERSM

2.2.1 MERSM principle

The section proposes MERSM based on ERSM and MRSM to deal with the dynamic probabilistic design of multi-component system with multi-failure modes. For multi-component system, MERSM is used to establish the extremum response surface models for the probabilistic analyses of many sub-components, and then many extremum response functions are coordinated to process the comprehensive probabilistic design of multi-component system with multi-failure modes.

The specific flow of the probabilistic design of multi-component system with multi-failure modes based on MERSM is summarized as follows:

1) Establish the finite element (FE) models for each component and each failure mode. Dynamic output responses of multiple components are acquired by deterministic dynamic analysis with respect to random input variables in time domain [0, T] based on the constraint conditions. The maximum response values of each component or failure mode are taken as the research target of the probabilistic analysis of multi-component system.

2) Structure multiple extremum response surface models by exploiting least square method [24, 25] in the light of extracting a small number of samples from random input variables and maximum response values of each component or failure mode.

3) Realize the comprehensive reliability analysis of whole multi-component system utilizing the multiple extremum response surface models fitted by extracting a number of linkage samples for multiple components and multiple failure modes with MC method [26, 27].

4) Analyze the sensitivity of the random input variables on the corresponding output responses, and then gain the influence level of the input random variables on the response of system.

As shown from the above analysis, MERSM could resolve the dynamic probabilistic analysis of multi-component system with multi-failure modes and make the difficult problem become simple. MC method is applied to linkage samples for multiple components and multiple failure modes. Linkage samples of MC method are defined as: multiple output responses are sampled at the same time, and the values of those output responses are compared with allowed values. Once one output response is higher than allowed value, the structural system is out of work.

2.2.2 MERSM model

The mathematical model of MERSM was established by building multiple extremum response surfaces models just like Eq. (1) simultaneously. With the reliability analysis of structure involving m ($m\in Z$) components and n ($n\in Z$) failure modes for each component, and assuming that $\boldsymbol{X}^{(ij)}$ is the random input variable vector of the jth failure mode in the ith component and $y^{(ij)}$ is the corresponding output variable, the relationship of $\boldsymbol{X}^{(ij)}$ and $y^{(ij)}$ is

$$y^{(ij)}\left(\boldsymbol{X}^{(ij)}\right)=f\left(\boldsymbol{X}^{(ij)}\right)\quad (i=1,\ 2,\ \cdots,\ m;\ j=1,\ 2,\ \cdots,\ n) \tag{6}$$

By the format of quadratic polynomial function, the above response surface function is rewritten,

$$y^{(ij)}\left(\boldsymbol{X}^{(ij)}\right)=A^{(ij)}+\boldsymbol{B}^{(ij)}\boldsymbol{X}^{(ij)}+\left(\boldsymbol{X}^{(ij)}\right)^{\mathrm{T}}\boldsymbol{C}^{(ij)}\boldsymbol{X}^{(ij)} \tag{7}$$

For multi-component system with multi-failure modes, the multi-extremum response surface model of this system is structured as

$$\begin{aligned}\boldsymbol{y}&=\left\{y^{(ij)}\left(\boldsymbol{X}^{(ij)}\right)\right\}_{i=1,\ 2,\ \cdots,\ m;\ j=1,\ 2,\ \cdots,\ n}\\&=\left\{\boldsymbol{A}^{(ij)}+\boldsymbol{B}^{(ij)}\boldsymbol{X}^{(ij)}+\left(\boldsymbol{X}^{(ij)}\right)^{\mathrm{T}}\boldsymbol{C}^{(ij)}\boldsymbol{X}^{(ij)}\right\}_{i=1,2,\cdots,m;\ j=1,2,\cdots,n}\end{aligned} \tag{8}$$

in which $\boldsymbol{y}$ denotes multi-extremum response surface model; $\boldsymbol{A}^{(ij)}$, $\boldsymbol{B}^{(ij)}$ and $\boldsymbol{C}^{(ij)}$ are the constant term, the vector of linear term and the matrix of quadratic term of the jth failure mode in the ith component, respectively. The undetermined coefficients are acquired on the basis of least square method when the number of samples is enough. Thus the vector $\boldsymbol{D}^{(ij)}$ of the undetermined coefficients is formed by

$$\boldsymbol{D}^{(ij)}=\left[a^{(ij)}\ \ b_1^{(ij)}\ \ b_2^{(ij)}\ \ \ldots\ b_k^{(ij)}\ \ c_{11}^{(ij)}\ \ c_{21}^{(ij)}\ \ c_{22}^{(ij)}\ \ \cdots\ \ c_{kk}^{(ij)}\right]^{\mathrm{T}} \tag{9}$$

where k is the number of input random variables.

For each response surface function, the undetermined coefficient vector $\boldsymbol{D}^{(ij)}$ are gained by

$$\boldsymbol{D}^{(ij)}=\left[\left(\boldsymbol{X}^{(ij)}\right)^{\mathrm{T}}\boldsymbol{X}^{(ij)}\right]^{-1}\left(\boldsymbol{X}^{(ij)}\right)^{\mathrm{T}}\left(y^{(ij)}\left(X^{(ij)}\right)\right) \tag{10}$$

From Eq. (10), we can obtain the undetermined coefficients of Eq. (8), i.e., multi-extremum response surface mathematical model of multi-failure modes for multi-component system.

3 Reliability sensitivity analysis

3.1 Reliability analysis of MERSM

The basic steps of MERSM reliability analysis are as follows:

1) The output responses of multi-component

and multi-failure mode are gained by MC method to carry out a large amount of linkage sampling on multi-extremum response surface model of multi-component and multi-failure mode just like Eq. (8).

2) When $y_{\max}^{(ij)}$ is the maximum output value of each component and each failure mode, the limit state function of multi-extremum response surface is established as

$$\boldsymbol{H}=\left\{\boldsymbol{H}^{(ij)}\left(\boldsymbol{X}^{(ij)}\right)\right\}=\left\{y_{\max}^{(ij)}-\boldsymbol{y}\right\}=\left\{y_{\max}^{(ij)}-y^{(ij)}\left(\boldsymbol{X}^{(ij)}\right)\right\}=\left\{y_{\max}^{(ij)}-\boldsymbol{A}^{(ij)}-\boldsymbol{B}^{(ij)}\boldsymbol{X}^{(ij)}-\left(\boldsymbol{X}^{(ij)}\right)^{\mathrm{T}}\boldsymbol{C}^{(ij)}\boldsymbol{X}^{(ij)}\right\} \quad (11)$$

where i=1, 2, ⋯, m; j=1, 2, ⋯, n. Equation (11) is rewritten as

$$\left\{\boldsymbol{H}^{(ij)}\left(\boldsymbol{X}^{(ij)}\right)\right\}=\left\{y_{\max}^{(ij)}-a^{(ij)}-\sum_{p=1}^{k}b_p^{(ij)}\boldsymbol{X}_p^{(ij)}-\sum_{p=1}^{k-1}\sum_{q=p+1}^{k}c_{pq}^{(ij)}\boldsymbol{X}_p^{(ij)}\boldsymbol{X}_p^{(ij)}-\sum_{p=1}^{k}c_{pq}^{(ij)}\left(\boldsymbol{X}_p^{(ij)}\right)^2\right\} \quad (12)$$

in which $\boldsymbol{X}_p^{(ij)}$ and $\boldsymbol{X}_q^{(ij)}$ denote the pth value and the qth value of the input variable $\boldsymbol{X}$ in the jth failure mode of the ith component of the structure, respectively; $a^{(ij)}$, $b_p^{(ij)}$, $c_{pq}^{(ij)}$ and $c_{pp}^{(ij)}$ respectively denote the undetermined coefficients of constant term, linear term, quadratic term.

3) As known in Eq. (12), $\boldsymbol{H}^{(ij)}(\boldsymbol{X}^{(ij)})\leq 0$ denotes the failure of the structure; while $\boldsymbol{H}^{(ij)}(\boldsymbol{X}^{(ij)})>0$ expresses that the structure is secure. The comprehensive reliability degree of structure is calculated with sampling statistics.

3.2 Sensitivity analysis of MERSM

The purpose of sensitivity analysis is to study the influence of random input variables on the reliability of structure. The sensitivity reflects the influence level of the variation of random variables on failure probability.

If $\boldsymbol{H}$ obeys a normal distribution and random input variables are mutually independent, by MC method, the failure probability is as follows:

$$P_f=1-\Phi\left(\frac{\boldsymbol{\mu}_{\mathrm{H}}}{\sqrt{\boldsymbol{D}_{\mathrm{H}}}}\right) \quad (13)$$

in which $\Phi(\cdot)$ is the standard normal distribution function; $\boldsymbol{\mu}_{\mathrm{H}}$ is the mean matrix of the limit state function and $\boldsymbol{D}_{\mathrm{H}}$ is the variance matrix of the limit state function. $\boldsymbol{\mu}_{\mathrm{H}}$ and $\boldsymbol{D}_{\mathbf{H}}$ are denoted by

$$\begin{cases}\boldsymbol{E}[H]=\boldsymbol{\mu}_H\left(\mu_1^{11}\ \ \mu_2^{11}\ \ \cdots\ \ \mu_k^{11}\cdots\ \ \mu_1^{mn}\ \ \cdots\ \ \mu_k^{mn}\right.\\ \qquad\left.D_1^{11}\ \ \cdots\ \ D_k^{11}\ \ \cdots\ \ D_1^{mn}\ \ \cdots\ \ D_k^{mn}\right)\\ \boldsymbol{D}[H]=\boldsymbol{D}_H\left(\mu_1^{11}\ \ \mu_2^{11}\ \ \cdots\ \ \mu_k^{11}\cdots\ \ \mu_1^{mn}\ \ \cdots\ \ \mu_k^{mn}\right.\\ \qquad\left.D_1^{11}\ \ \cdots\ \ D_k^{11}\ \ \cdots\ \ D_1^{mn}\ \ \cdots\ \ D_k^{mn}\right)\end{cases} \quad (14)$$

The sensitivities of failure probability of the random input variables are obtained by

$$\begin{cases}\dfrac{\partial P_f}{\partial\boldsymbol{\mu}}=\dfrac{1}{k}\displaystyle\sum_{i=1}^{k}\frac{\partial\boldsymbol{P}_f}{\partial\boldsymbol{\mu}_{X_i}}=\frac{\partial(1-P_r)}{\partial\boldsymbol{\mu}}\\ \dfrac{\partial P_f}{\partial\boldsymbol{D}}=\dfrac{1}{k}\displaystyle\sum_{i=1}^{k}\frac{\partial\boldsymbol{P}_f}{\partial\boldsymbol{D}_{X_i}}=\frac{\partial(1-P_r)}{\partial\boldsymbol{D}}\end{cases} \quad (15)$$

Equation (15) is rewritten as

$$\begin{cases}\dfrac{\partial P_r}{\partial\boldsymbol{\mu}}=\dfrac{\partial P_r}{\partial\left(\dfrac{\boldsymbol{\mu}_H}{\sqrt{\boldsymbol{D}_H}}\right)}\left(\dfrac{\partial\left(\dfrac{\boldsymbol{\mu}_H}{\sqrt{\boldsymbol{D}_H}}\right)}{\partial\boldsymbol{\mu}_H}\dfrac{\partial\boldsymbol{\mu}_H}{\partial\boldsymbol{\mu}}+\dfrac{\partial\left(\dfrac{\boldsymbol{\mu}_H}{\sqrt{\boldsymbol{D}_H}}\right)}{\partial\boldsymbol{D}_H}\dfrac{\partial\boldsymbol{D}_H}{\partial\boldsymbol{\mu}}\right)\\ \dfrac{\partial P_r}{\partial\boldsymbol{D}}=\dfrac{\partial P_r}{\partial\left(\dfrac{\boldsymbol{\mu}_H}{\sqrt{\boldsymbol{D}_H}}\right)}\left(\dfrac{\partial\left(\dfrac{\boldsymbol{\mu}_H}{\sqrt{\boldsymbol{D}_H}}\right)}{\partial\boldsymbol{\mu}_H}\dfrac{\partial\boldsymbol{\mu}_H}{\partial\boldsymbol{D}}+\dfrac{\partial\left(\dfrac{\boldsymbol{\mu}_H}{\sqrt{\boldsymbol{D}_H}}\right)}{\partial\boldsymbol{D}_H}\dfrac{\partial\boldsymbol{D}_H}{\partial\boldsymbol{D}}\right)\end{cases} \quad (16)$$

where related parameters are determined by

$$\begin{cases}\dfrac{\partial\left(\dfrac{\boldsymbol{\mu}_H}{\sqrt{\boldsymbol{D}_H}}\right)}{\partial\boldsymbol{\mu}_H}=\dfrac{1}{\sqrt{D_H}},\dfrac{\partial\left(\dfrac{\boldsymbol{\mu}_H}{\sqrt{\boldsymbol{D}_H}}\right)}{\partial D_H}=-\dfrac{\boldsymbol{\mu}_H}{2}\boldsymbol{D}_H^{-\frac{3}{2}}\\ \dfrac{\partial\boldsymbol{\mu}_H}{\partial\boldsymbol{\mu}}=\left[\dfrac{\partial\boldsymbol{\mu}_H}{\partial\mu_1^{11}}\ \dfrac{\partial\boldsymbol{\mu}_H}{\partial\mu_2^{11}}\ \cdots\ \dfrac{\partial\boldsymbol{\mu}_H}{\partial\mu_k^{11}}\ \cdots\ \dfrac{\partial\boldsymbol{\mu}_H}{\partial\mu_1^{mn}}\ \cdots\ \dfrac{\partial\boldsymbol{\mu}_H}{\partial\mu_k^{mn}}\right]\\ \dfrac{\partial\boldsymbol{\mu}_H}{\partial\boldsymbol{D}}=\left[\dfrac{\partial\boldsymbol{\mu}_H}{\partial D_1^{11}}\ \dfrac{\partial\boldsymbol{\mu}_H}{\partial D_2^{11}}\ \cdots\ \dfrac{\partial\boldsymbol{\mu}_H}{\partial D_k^{11}}\ \cdots\ \dfrac{\partial\boldsymbol{\mu}_H}{\partial D_1^{mn}}\ \cdots\ \dfrac{\partial\boldsymbol{\mu}_H}{\partial D_k^{mn}}\right]\\ \dfrac{\partial\boldsymbol{D}_H}{\partial\boldsymbol{\mu}}=\left[\dfrac{\partial\boldsymbol{D}_H}{\partial\mu_1^{11}}\ \dfrac{\partial\boldsymbol{D}_H}{\partial\mu_2^{11}}\ \cdots\ \dfrac{\partial\boldsymbol{D}_H}{\partial\mu_k^{11}}\ \cdots\ \dfrac{\partial\boldsymbol{D}_H}{\partial\mu_1^{mn}}\ \cdots\ \dfrac{\partial\boldsymbol{D}_H}{\partial\mu_k^{mn}}\right]\\ \dfrac{\partial\boldsymbol{D}_H}{\partial\boldsymbol{D}}=\left[\dfrac{\partial\boldsymbol{D}_H}{\partial D_1^{11}}\ \dfrac{\partial\boldsymbol{D}_H}{\partial D_2^{11}}\ \cdots\ \dfrac{\partial\boldsymbol{D}_H}{\partial D_k^{11}}\ \cdots\ \dfrac{\partial\boldsymbol{D}_H}{\partial D_1^{mn}}\ \cdots\ \dfrac{\partial\boldsymbol{D}_H}{\partial D_k^{mn}}\right]\end{cases} \quad (17)$$

4 Case study

High pressure turbine blisk of an aeroengine is selected as the object of study in this section. To

simulate the working state of aeroengine, the flight profile and computing range are chosen from aeroengine start to cruise state [18–22, 28, 29]. Nickel-base superalloys with different parameters are selected as the materials of blade and disk. The thermal-structure coupling method is utilized to analyze the blisk structure under the consideration of the nonlinearity of material property and the dynamics of temperature and rotational speed. The load spectrums of temperature T and rotational speed ω are shown in Table 1.

Table 1 Temperature and speed value change with time

Time, t/s	Temperature, T/°C	Rotate speed, ω/(rad·s^{-1})
0	20	0
0.1	200	460
10	300	498
95	400	627
100	500	725
130	600	800
140	700	930
150	800	980
160	900	1168
165	1000	1168
200	1100	950
215	1200	950

4.1 Finite element model

Aeroengine turbine is a typical cyclic symmetric structure, so a single blisk is selected as the object of simulation. Cooling hole of the blade, fillet and convex platform of the disk are simplified to build the FE models of turbine blade and disk as shown in Figure 2. The FE model of the blade consists of hexahedron with the number of elements 456 and the FE model of the blade consists of tetrahedron with the number of elements 7302.

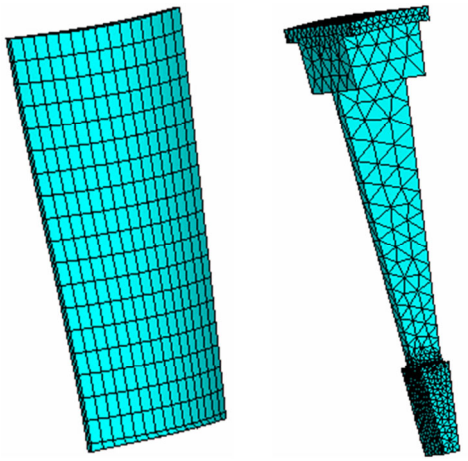

(a) (b)

Figure 2 FE models of turbine blade and disk: (a) FE model of turbine blade; (b) FE model of turbine disk

4.2 Random input variables selection

Some parameters are reasonably selected as random input variables as shown in Table 2, including rotational speed ω, gas temperature T, disk's material density ρ_1, blade's material density ρ_2, disk's elastic modulus E_1 and blade's elastic modulus E_2.

4.3 Deterministic analysis on blisk

Considering the dynamics of rotational speed and gas temperature and the nonlinearity of material property, the deterministic analysis of blisk was completed by thermal-structure coupling analysis method within the time domain [0, 215]. Blisk structure is in the temperature field without heat resource. 3-dimensional heat conduction equation (Eq. (18)) was built according to Fourier thermal conductivity law [30, 31] and energy conservation law [32]. Thermal analysis of blisk was finished with the heat convection-based Newton cooling equation (Eq. (19)) and the initial condition (Eq. (20)). The data of thermal analysis are transferred into the surfaces of blisk structure. The

Table 2 Distribution characteristics of random input variables

Random input variable	Distribution	Mean	Standard deviation	Correlation
Rotating speed, ω/(rad·s^{-1})	Normal	1168	10.81	—
Gas temperature, T/°C	Normal	1200	10.96	—
Disk's density, ρ_1/(kg·m^{-3})	Normal	8240	28.71	—
Blade's density, ρ_2/(kg·m^{-3})	Normal	8570	29.27	ρ_2=1.040ρ_1
Disk's elastic modulus, E_1/Pa	Normal	2.05×10^{11}	1.43×10^{5}	—
Blade's elastic modulus, E_2/Pa	Normal	2.02×10^{11}	1.42×10^{5}	E_2=0.988 E_1

thermal-structure coupling analysis was executed from the output responses of structure by finite element formula (shape function of tetrahedron and hexahedron, geometric equation and constitutive equations) [33–35].

$$c\rho\frac{\partial T}{\partial t}=\frac{\partial}{\partial x}(k\frac{\partial T}{\partial x})+\frac{\partial}{\partial y}(k\frac{\partial T}{\partial y})+\frac{\partial}{\partial z}(k\frac{\partial T}{\partial z}) \tag{18}$$

where $k=k(x, y, z)$ is the thermal conductivity on the point (x, y, z); c and ρ are heat capacity and material density, respectively.

$$q^{*}=h_{\mathrm{f}}(T_{\mathrm{S}}-T_{\mathrm{B}}) \tag{19}$$

in which h_{f}, T_{S} and T_{B} are the convective coefficient of heat transfer, surface temperature and environment temperature.

$$T_{t=0}(x,y,z)=T_0(x,y,z) \tag{20}$$

in which T_0 is the initial temperature of structure.

From the deterministic analysis, the change curves of blade's and disk's deformations and stresses with time are shown in Figure 3. In Figure 3, u_{b}, u_{d}, σ_{b} and σ_{d} indicate blade deformation, disk deformation, stress on blade and stress on disk, respectively (similarly hereinafter).

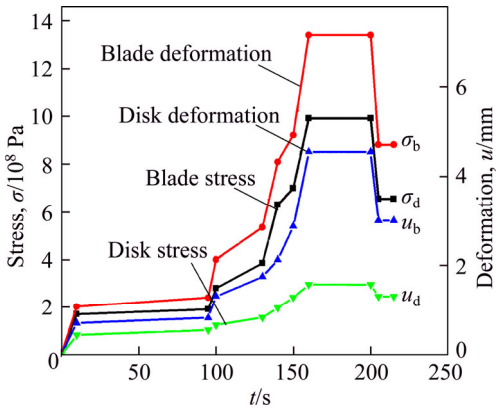

Figure 3 Variations of deformations and stresses with time for turbine blade and disk

As shown in Figure 3, the maximum deformations and stresses of blade and disk are acquired simultaneously at the time domain [160, 200]. The time point t=200 s is selected as the dangerous point. The dangerous point should be regarded as the computing point of reliability analysis because the safety at t=200 s makes aeroengine secure in the period of overall flight. Thus, the nephograms of the deformations and stresses of blade and disk are shown in Figure 4.

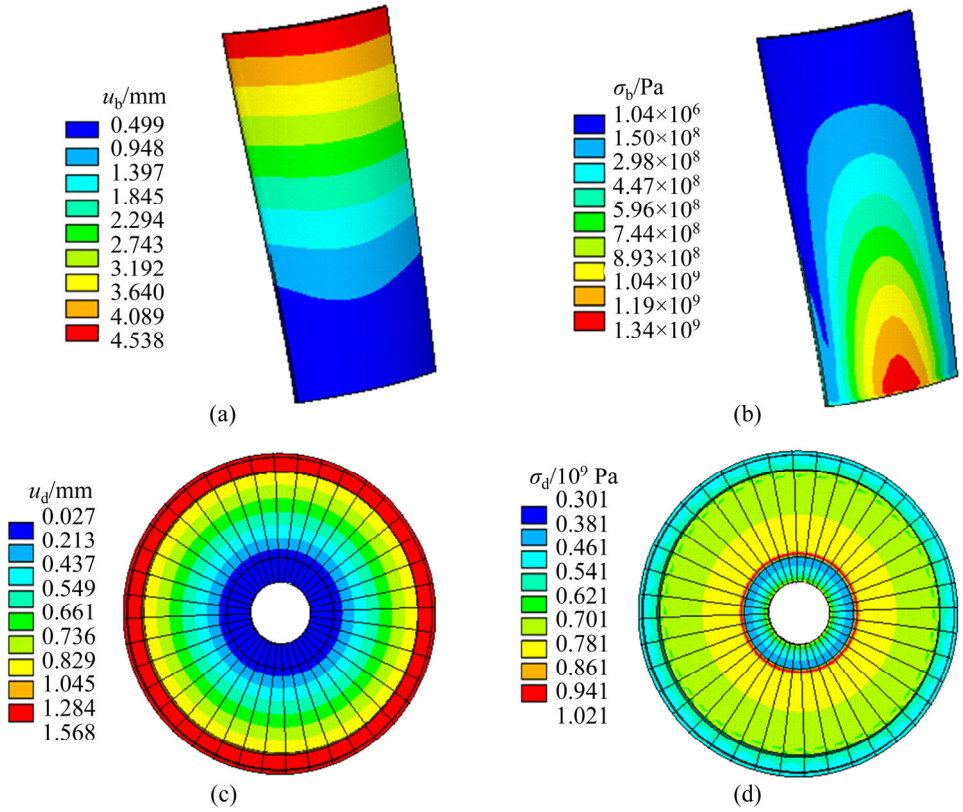

Figure 4 Radial distributions of deformations and stresses of turbine blade and disk: (a) Radial deformation distribution of turbine blade; (b) Radial stress distribution on turbine blade; (c) Radial deformation distribution of turbine disk; (d) Radial stress distribution on turbine disk

4.4 Reliability analysis of turbine blisk

By the design of experiments based on MC simulation with Latin Hypercube sampling method, 30 groups of simples were extracted at t=200 s on the foundation of thermal-structure coupling analysis. These samples were used to fit multiple extremum response surface models for blade deformation, blade stress, disk deformation and disk stress, respectively. Four extremum response surface models established are shown in Eq. (21).

$$\boldsymbol{y}(\rho,E,T,w)=\begin{cases} y^{(11)}=4.538\times10^{-3}-2.803\times10^{-12}\rho_1-3.220\times10^{-9}E_1+2.097\times10^{-12}T+8.402\times10^{-5}-1.885\times10^{-12}\rho_1^2+6.337\times10^{-13}E_1^2+2.164\times10^{-12}T^2+3.889\times10^{-7}\omega^2-7.041\times10^{-13}\rho_1E_1-2.155\times10^{-12}\rho_1T-3.458\times10^{-12}\rho_1\omega-2.329\times10^{-12}E_1T-6.278\times10^{-11}E_1\omega-1.624\times10^{-12}T\omega \\ y^{(12)}=1.339\times10^{9}-2.187\rho_1-2.485E_1+1.137T+2.479\times10^{7}\omega-1.188\rho_1^2+1.309E_1^2+1.377T^2+1.147\times10^{5}\omega^2+2.457\rho_1E_1-2.520\rho_1T-3.202\rho_1\omega-1.431E_1T+2.642E_1\omega-0.363T\omega \\ y^{(21)}=1.568\times10^{-3}-4.025\times10^{-13}\rho_1-4.692\times10^{-10}E_1+3.049\times10^{-13}T+1.224\times10^{-5}\omega-2.821\times10^{-13}\rho_1^2+9.549\times10^{-14}E_1^2+3.187\times10^{-13}T^2+5.667\times10^{-8}\omega^2-1.088\times10^{-13}\rho_1E_1-3.035\times10^{-13}\rho_1T-4.954\times10^{-13}\rho_1\omega-3.425\times10^{-13}E_1T-9.153\times10^{-12}E_1\omega-2.364\times10^{-13}T\omega \\ y^{(22)}=9.906\times10^{8}-1.294\rho_1+0.558E_1-0.545T+1.834\times10^{-7}\omega-1.215\rho_1^2-0.458E_1^2-0.238T^2+8.490\times10^{4}\omega^2+0.695\rho_1E_1-0.166\rho_1T-5.803\times10^{-2}\rho_1\omega-1.351E_1T-1.320E_1\omega-0.868T\omega \end{cases} \tag{21}$$

where $y^{(11)}$, $y^{(12)}$, $y^{(21)}$ and $y^{(22)}$ are the extremum response surface models of blade deformation, blade stress, disk deformation and disk stress, respectively.

According to the experience of engineering, $y_{\max}^{(11)}$ =4.78×10^{-3} m, $y_{\max}^{(12)}$ =1.41×10^{9} Pa, $y_{\max}^{(21)}$ = 1.64×10^{-3} m and $y_{\max}^{(22)}$=1.04×10^{9} Pa are selected as the maximum allowable deformations and stresses of turbine blade and turbine disk, respectively. The four extremum response surface models were employed in the reliability analysis instead of finite element models by 10000 times simulations using MC simulation-based Latin Hypercube sampling method. Under confidence level 0.95, the simulation samples and frequency distributions of maximum deformations and stresses are shown in Figures 5 and 6, respectively. In Figures 5 and 6, y^{11}, y^{12}, y^{21} and y^{22} are the maximum deformations and stresses of blade and disk, respectively. The results reveal that the comprehensive reliability of blisk is 0.9904.

From Figures 5 and 6, all the output responses follow normal distribution, in which the mean and standard deviations of blade maximum deformation $y^{(11)}$, blade maximum stress $y^{(12)}$, disk maximum deformation $y^{(21)}$ and disk maximum stress $y^{(22)}$ are 4.538×10^{-3} m, 1.339×10^{9} Pa, 1.568×10^{-3} m, 9.907×10^{8} Pa, and 8.395×10^{-5} m, 2.476×10^{7} Pa, 1.223×10^{-5} m, 1.8333×10^{7} Pa, respectively. In addition, it is also revealed that the comprehensive reliability degree of turbine blisk is 0.9904 through reliability analysis.

4.5 Sensitivity analysis of turbine blisk

Sensitivity analysis of turbine blisk is used to determine the comprehensive effect level of random input variables (material density, elasticity modulus, temperature, rotational speed and so on) on output parameters (the deformation and stress of turbine blade and disk), and further estimate whether the random input variables hold important impact on whole structure failure.

MC method is applied to carrying out linkage sampling for four extremum response surface models of turbine blisk Eq. (21). The comprehensive failure probability is obtained by using Eq. (12). And then the sensitivity degree and impact probabilities of turbine blisk are calculated by Eqs. (13)–(17). Through the sensitivity analysis of turbine blade and disk, sensitivity degree and impact probability of random input variables are shown in Figure 7. Sensitivity degrees in the histogram and impact probability in pie chart are comprehensive sensitivity degree and comprehensive impact probability of random input variables on turbine blisk, respectively.

As shown in Figure 7, the sensitivities of random input variables have positive and negative

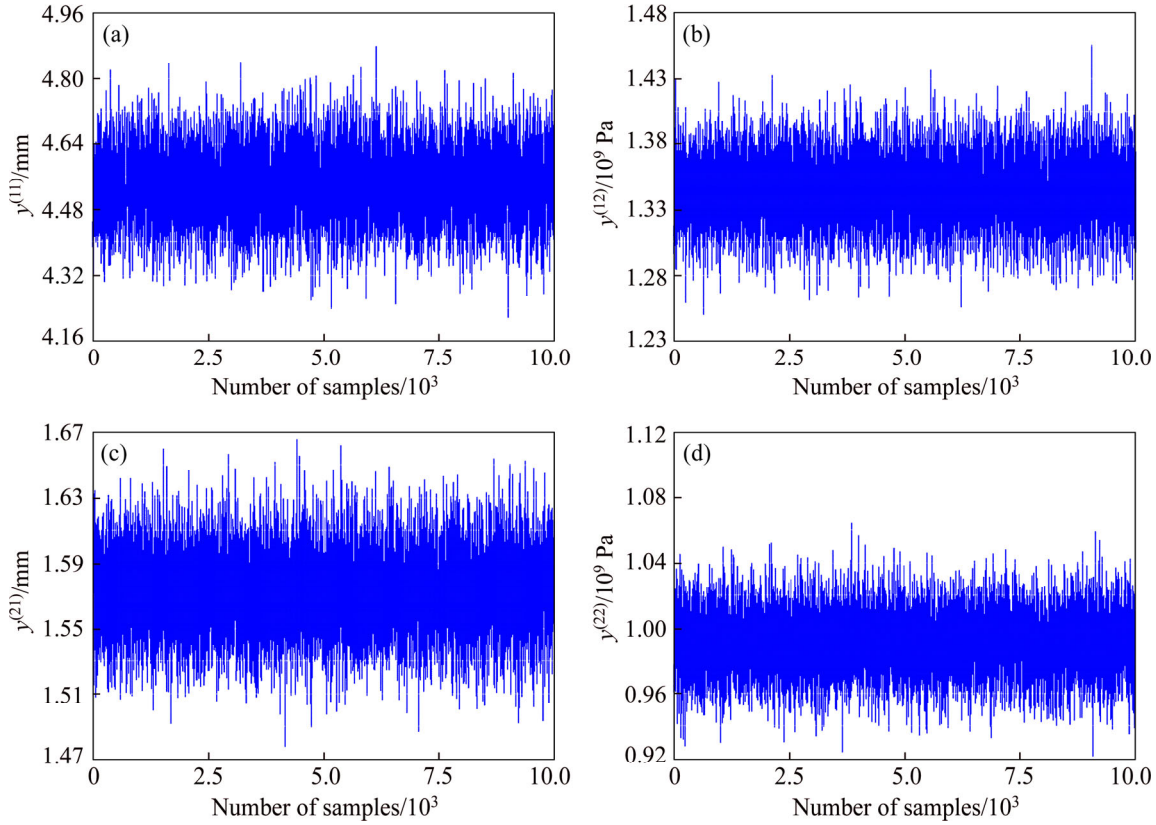

Figure 5 Deformation and stress simulation history of blade, disk: (a) Blade deformation; (b) Blade stress; (c) Disk deformation; (d) Disk stress

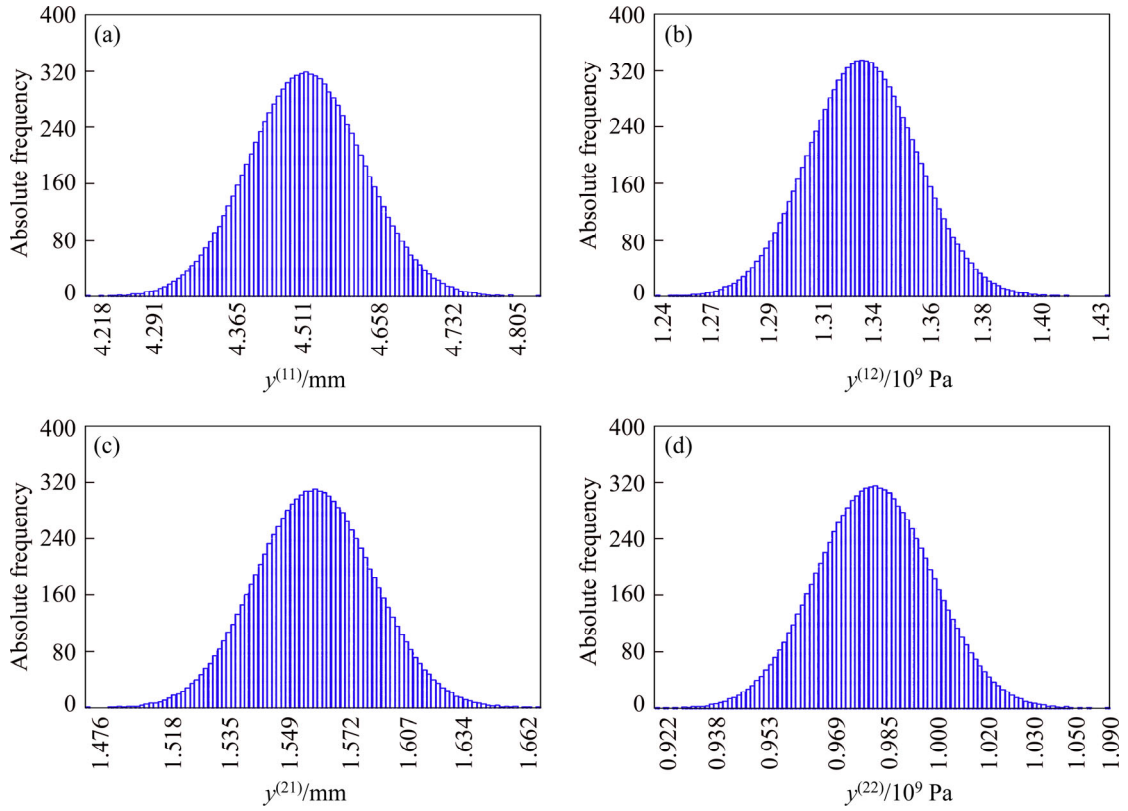

Figure 6 Deformation and stress frequency distribution of blade and disk: (a) Frequency distribution of blade deformation; (b) Frequency distribution of blade stress; (c) Frequency distribution of disk deformation; (d) Frequency distribution of disk stress

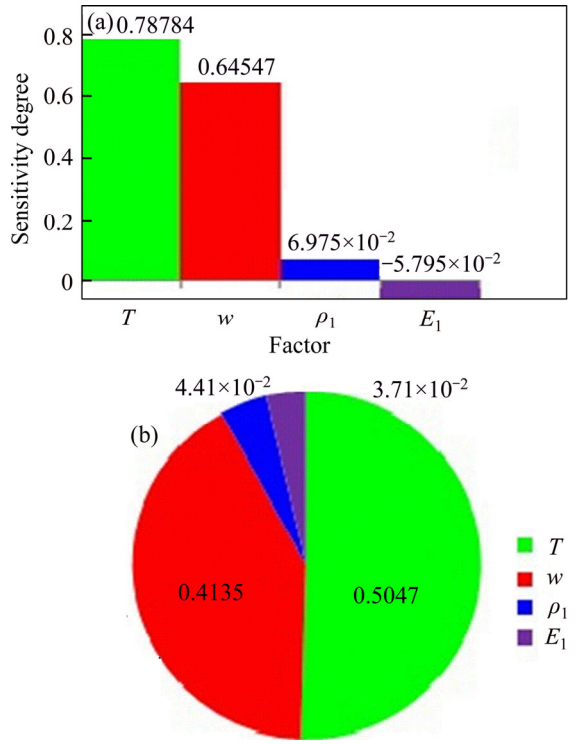

Figure 7 Sensitivity results of random input variables: (a) Sensitivity degree; (b) Influencing probability

values. Positive value reveals that output responses produce a positive variety with random input variables, while negative values denote that output response inversely changes with random input variable. Temperature T and rotate speed ω play an important role because of larger sensitivities (0.7878 and 0.6455) and effect probabilities (0.5047 and 0.4135). The sensitivities of density ρ_1 and elasticity modulus E_1 are 0.06975 and –0.05795 and their effect probabilities are 0.0441 and 0.0371 respectively. As illustrated by the sensitivity analysis, the increase of temperature T, rotate speed ω and material density ρ_1 promote the increase of deformation and stress. Nevertheless, the increase of elasticity modulus restrains the increase of the deformation and stress of turbine blade and disk. Therefore, in blisk design of the aeroengine high-pressure turbine, temperature T and rotate speed ω are advised to control with priority. Large elasticity modulus is conductive to the design of blisk.

4.6 MERSM validation

To verify the validity and feasibility of the proposed MERSM, MC method, ERSM and MERSM were used to the reliability analysis of aeroengine turbine blisk based on random input variables in Table 1 and the same computing environment. Computational time by three method is shown in Table 3 and reliability analysis results of blisk at $y_{\max}^{(11)}$=4.78 mm, $y_{\max}^{(12)}$=1.41×10^9 Pa, and $y_{\max}^{(21)}$=1.64 mm, $y_{\max}^{(22)}$=1.04×10^9 Pa are listed in Table 4.

4.7 Discussion

As demonstrated by Table 3, the computational time of MERSM is far less than ERSM and MC method, because MERSM only spends 0.182 s, while ERSM and MC methods cost 1.158 s and 1754394 s under 1000 times simulations, respectively. In addition, the computational efficiency of MERSM becomes more obvious with the increasing of simulations. For instance, the computing time of MERSM is 1/5 that of ERSM under 100 simulations while MERSM is about 1/8 that of ERSM under 100000 simulations, because MERSM and ERSM consume 0.127 s and 0.635 s for 100 simulations and 1.575 s and 12.537 s for 100000 simulations, respectively. For fitting time, 15.32 s for the proposed MERSM is far less than 4.76 s for ERSM. The results reveal the high computational efficiency of the developed MERSM.

As shown in Table 4, the computational precision of MERSM is higher than that of ERSM and almost consistent with that of MC method. Especially, the computational accuracy of MERSM is averagely improved by 0.94% to ERSM under 100 simulations. Additionally, the MERSM

Table 3 Computational time of three methods for blisk reliability analysis

Method	Fitting time/h	Computing time of different simulation numbers/h				
		100	1000	10000	100000	1000000
MC method	—	50.82	487.33	—	—	—
ERSM	15.32	1.76×10^{-4}	3.21×10^{-4}	7.26×10^{-4}	3.48×10^{-3}	—
MERSM	4.76	3.52×10^{-5}	5.05×10^{-5}	1.02×10^{-4}	4.38×10^{-4}	1.35×10^{-3}

Table 4 Results of blisk reliability analysis based on three methods

Number of simulations	Reliability/%			Precision/%		Improved precision/%
	MC method	ERSM	MERSM	ERSM	MERSM	
10^2	98.42	97.24	98.16	98.80	99.74	0.94
10^3	98.89	97.98	98.74	99.08	99.85	0.77
10^4	—	98.67	99.04	—	—	—
10^5	—	98.66	99.46	—	—	—
10^6	—	—	99.32	—	—	—

completes the calculation and addresses the reliability analysis problem of multi-component system with multi-failure modes that the ERSM and MC method almost unlikely achieve, when the number of simulations is larger than 1000 for MC method and 100000 for ERSM. The results indicate the high computational precision of the developed MERSM.

Though the above conclusions, it is supported that the MERSM reasonably processes the transients and multiple models of multi-component system with multi-failure modes, and thereby greatly improves the calculation speed and efficiency while keeping high computational precision.

5 Conclusions

The aim of this study is to propose multi-extremum response surface method (MERSM) for the time-varying probabilistic analysis of multi-component system with multi-failure modes with the emphasis on the solution of transients and multiple models. The dynamic reliability analysis of aeroengine turbine blisk is studied to validate the effectiveness and reasonability of the presented MERSM. From dynamic deterministic analysis of turbine blisk, the maximum deformations and stresses of blade and disk are 4.538 mm, 1.568 mm, 1.339×10^9 Pa and 9.906×10^9 Pa, respectively. The mathematical model of MERSM is demonstrated to be effective and reasonable (high computational efficiency and precision) in the time-varying probabilistic analysis of multi-component system with multi-failure modes, by the reliability analysis of an aeroengine turbine blisk with turbine disk and turbine blade with stress and deformation failures. The reliability analysis of turbine blisk reveals the comprehensive reliability degree 0.9904 when the maximum allowable deformations of blade and disk are 4.78 mm and 1.64 mm, and the maximum allowable stresses of blade and disk are 1.41×10^9 Pa and 1.04×10^9 Pa, respectively. Sensitivity analysis demonstrates that temperature T and rotational speed ω play important roles on the comprehensive reliability, while the material density and elasticity modulus are not too important. It is advised to consider temperature T and rotational speed ω with priority in blisk design. Through the comparison of methods, it is validated that MERSM holds high computational precision and efficiency for the reliability design of multi-component system with multi-failure mode on the premise of guarantee calculation precision, which reveals that MERSM can effectively handle the two key issues of transients and multiple models in dynamic probabilistic analysis of multi-component system.

References

[1] REED D A. Reliability of multi-component assemblages [J]. Reliability Engineering & System Safety, 1990, 27: 167–178.

[2] GASPAR B, NAESS A, LEIRA B J, SOARES C G. System reliability analysis by Monte Carlo based method and finite element structural models [J]. ASME Journal of Offshore Mechanics and Arctic Engineering, 2014, 136: 031603.

[3] FEI C W, BAI G C. Distributed collaborative response surface method for mechanical dynamic assembly reliability design [J]. Chinese Journal of Mechanical Engineering, 2013, 26: 1160–1168.

[4] BAI B, BAI G C, LI C. Application of multi-stage multi-objective multi-disciplinary agent model based on dynamic substructural method in Mistuned Blisk [J]. Aerospace Science and Technology, 2015, 469: 104–115.

[5] SINGH P K, JAIN S C, JAIN P K. Advanced optimal tolerance design of mechanical assemblies with interrelated dimension chains and process precision limits [J]. Computers in Industry, 2005, 56: 179–194.

[6] TEISSANDIER D, COUETARD Y, GERARD A. A computer aided tolerance model: Proportioned assembly clearance volume [J]. Computer-Aided Design, 1999, 31:

805–817.

[7] LI D Q, JIANG S H, WU S B, ZHOU C B, ZHANG L M. Modeling multivariate distributions using Monte Carlo simulation for structural reliability analysis with complex performance function [J]. Proceedings of the Institution of Mechanical Engineers Part O-Journal of Risk and Reliability, 2013, 227: 109–118.

[8] ZHANG H, DAI H Z, BEER M, WANG W. Structural reliability analysis on the basis of small samples: An interval quasi-Monte Carlo method [J]. Mechanical Systems and Signal Processing, 2013, 37: 137–151.

[9] SHAHI M, MAZINAN A H. Monte-Carlo based cascade control approach with focus on real overactuated space systems [J]. Journal of Central South University, 2017, 23(12): 2171–3182.

[10] DONG H K, SANG G L. Reliability analysis of offshore wind turbine support structures under extreme ocean environmental loads [J]. Renewable Energy, 2014, 26: 161–166.

[11] KAYMAZ C A. Mcmahon, a response surface method based on weighted regression for structural reliability analysis [J]. Probabilistic Engineering Mechanics, 2005, 20: 11–17.

[12] AI C M, WU A X, WANG Y M, HOU C L. Optimization and mechanism of surfactant accelerating leaching test [J]. Journal of Central South University, 2016, 23(5): 1032–1039.

[13] ZHANG C Y, BAI G C. Extremum response surface method of reliability analysis on two-link flexible robot manipulator [J]. Journal of Central South University, 2012, 19(1): 101–107.

[14] REN Y, BAI G C. New neural network response surface methods for reliability analysis [J]. Chinese Journal of Aeronautics, 2011, 1: 25–31.

[15] ZHANG D, TANG S, CHE J. Concurrent subspace design optimization and analysis of hypersonic vehicles based on response surface models [J]. Aerospace Science and Technology, 2015, 42: 39–49.

[16] GUO Z W, BAI G C. Application of least squares support vector machine for regression to reliability analysis [J]. Chinese Journal of Aeronautics, 2009, 22: 160–166.

[17] FEI C W, TANG W Z, BAI G C. Novel method and model for dynamic reliability optimal design of turbine blade deformation [J]. Aerospace Science and Technology, 2014, 39: 588–595.

[18] FEI C W, TANG W Z, BAI G C. Nonlinear dynamic probabilistic design of turbine disk-radial deformation using extremum response surface method-based support vector machine of regression [J]. Proceedings of IME Part G-Journal of Aerospace Engineering, 2015, 229: 290–300.

[19] RABI B R M, NAGARA P. Finite element model updating of a space vehicle first stage motor based on experimental test results [J]. Aerospace Science and Technology, 2015, 45: 422–430.

[20] FEI C W, BAI G C. Nonlinear dynamic probabilistic analysis for turbine casing radial deformation based on extremum response surface method-based support vector machine [J]. Journal of Computational and Nonlinear Dynamics, 2013, 8: 041004.

[21] BAI B, BAI G C. Dynamic probabilistic analysis of stress and deformation for bladed disk assemblies of aeroengine [J]. Journal of Central South University, 2014, 21(10): 3722–3735.

[22] FEI C W, BAI G C. Distributed collaborative extremum response surface method for mechanical dynamic assembly reliability analysis [J]. Journal of Central South University, 2013, 20(9): 2414–2422.

[23] ZHAI X, FEI C W, WANG J J, WANG J J. Reliability sensitivity analysis of HTP blade-tip radial running clearance using multiply response surface model [J]. Journal of Central South University, 2014, 21(12): 4368–4377.

[24] HAMPTON J, DOOSTAN A. Coherence motivated sampling and convergence analysis of least squares polynomial Chaos regression [J]. Computer Methods in Applied Mechanics and Engineering, 2015, 290: 73–97.

[25] LINDER D F, REMPALA G A. Bootstrapping least-squares estimates in biochemical reaction networks [J]. Journal of Biological Dynamics, 2015(9): 125–146.

[26] CHEN G H, LI Q. Markov chain Monte Carlo sampling based terahertz holography image denoising [J]. Applied Optics, 2015(54): 4345–4351.

[27] DOUCET A, GODSILL S, ANDRIEU C. On sequential Monte Carlo sampling methods for Bayesian filtering [J]. Statistics and Computing, 2000(10): 197–208.

[28] KYPUROS J A, MELCHER K J. A reduced model for prediction of thermal and rotational effects on turbine tip clearance [R]. NASA/TM-20030212226, 2003.

[29] LATTIME S B, STEINETZ B M, ROBBIE M G. Test rig for evaluating active turbine blade tip clearance control concepts [J]. Journal of Propulsion and Power, 2005, 21: 552–563.

[30] GRUBER C, LESNE A. Hamiltonian model of heat conductivity and Fourier law [J]. Statistical Mechanics and its Applications, 2005, 351: 358–372.

[31] RUELLE D. A mechanical model for Fourier's law of heat conduction [J]. Communications in Mathematical Physics, 2012, 311: 755–768.

[32] ROTH G A, AYDOGAN F. Derivation of new mass, momentum and energy conservation equations for two-phase flows [J]. Progress in Nuclear Energy, 2015, 80: 90–101.

[33] DEVLOO P R B, AYALA BRAVO C M A A, RYLO E C. Systematic and generic construction of shape functions for p-adaptive meshes of multidimensional finite elements [J]. Computer Methods in Applied Mechanics and Engineering, 2009, 198: 1716–1725.

[34] HASHINUCHI K. Basic formulations for elastoplastic constitutive equations [J]. Elastoplasticity Theory, 2014, 69: 131–166.

[35] FOERCH R, BESSON J, CAILLETAUD G, DILVIN P. Polymorphic constitutive equations in finite element codes [J]. Computer Methods in Applied Mechanics and Engineering, 1997, 141: 355–372.

(Edited by YANG Hua)

中文导读

多构件结构的多失效模式动态可靠性分析

摘要：针对多构件多失效模式系统可靠性分析中计算效率和计算精度较差的问题，提出了多重极值响应面法，多重极值响应面是基于二次多项式响应面函数建立的多重极值响应面方程。基于热-结构耦合技术，考虑材料属性的非线性和气体载荷、气体温度、转速的瞬态性，对航空发动机叶盘双构件进行动态可靠性分析，得到其变形和应力的可靠性。结果显示：当叶片-轮盘结构的允许变形量、许用应力分别为 4.78 mm、1.41×10^9 Pa、1.64 mm 和 1.04×10^9 Pa 时，结构的综合可靠度为 0.9904。此外，燃气温度和转速对系统的综合可靠性影响较大。通过对比表明，MERSM 在可靠性分析计算中具有较高的计算精度和速度，计算精度满足工程设计要求。本文解决了具有多失效模式的多构件系统在瞬态和耦合时动态可靠性分析的困难。

关键词：可靠性分析；多重极值响应面法；多构件；多失效模式